Subscriber access provided by NATIONAL CHIAO TUNG UNIV

Article

High-bandwidth green semipolar (20-21) InGaN/GaN micro light-emitting diodes for visible light communication

Sung-Wen Huang Chen, Yu-Ming Huang, Yun-Han Chang, Yue Lin, Fang-Jyun Liou, Yu-Chien Hsu, Jie Song, Joowon Choi, Chi-Wai Chow, Chien-Chung Lin, Ray-Hua Horng, Zhong Chen, Jung Han, Tingzhu Wu, and Hao-Chung Kuo

ACS Photonics, **Just Accepted Manuscript** • DOI: 10.1021/acsphotonics.0c00764 • Publication Date (Web): 04 Jul 2020

Downloaded from pubs.acs.org on July 9, 2020

Just Accepted

“Just Accepted” manuscripts have been peer-reviewed and accepted for publication. They are posted online prior to technical editing, formatting for publication and author proofing. The American Chemical Society provides “Just Accepted” as a service to the research community to expedite the dissemination of scientific material as soon as possible after acceptance. “Just Accepted” manuscripts appear in full in PDF format accompanied by an HTML abstract. “Just Accepted” manuscripts have been fully peer reviewed, but should not be considered the official version of record. They are citable by the Digital Object Identifier (DOI®). “Just Accepted” is an optional service offered to authors. Therefore, the “Just Accepted” Web site may not include all articles that will be published in the journal. After a manuscript is technically edited and formatted, it will be removed from the “Just Accepted” Web site and published as an ASAP article. Note that technical editing may introduce minor changes to the manuscript text and/or graphics which could affect content, and all legal disclaimers and ethical guidelines that apply to the journal pertain. ACS cannot be held responsible for errors or consequences arising from the use of information contained in these “Just Accepted” manuscripts.

is published by the American Chemical Society. 1155 Sixteenth Street N.W., Washington, DC 20036

Published by American Chemical Society. Copyright © American Chemical Society. However, no copyright claim is made to original U.S. Government works, or works produced by employees of any Commonwealth realm Crown government in the course of their duties.

High-bandwidth green semipolar (20-21) InGaN/GaN micro light-emitting diodes for visible light communication

Sung-Wen Huang Chen, Yu-Ming Huang, Yun-Han Chang, Yue Lin, Fang-Jyun Liou, Yu-Chien Hsu, Jie Song, Joowon Choi, Chi-Wai Chow, Chien-Chung Lin, Ray-Hua Horng, Zhong Chen, Jung Han, Tingzhu Wu*, and Hao-Chung Kuo*

ABSTRACT: The light-emitting diode (LED) is among promising candidates of light sources in visible light communication (VLC); however, strong internal polarization fields in common *c*-plane LEDs, especially green LEDs result in low frequency and limited transmission performance. This study aims to overcome the limited 3-dB bandwidth of long-wavelength InGaN/GaN LEDs. Thus, semipolar (20-21) micro-LEDs (μLEDs) were fabricated through several improved approaches on epitaxy and chip processes. The μLED exhibits a 525 nm peak wavelength and good polarization performance. The highest 3-dB bandwidth up to 756 MHz and 1.5 Gbit/s data rate was achieved under a current density of 2.0 kA/cm^2. These results suggest a good transmission capacity of green semipolar (20-21) μLEDs in VLC applications.

KEYWORDS: semipolar GaN, micro light-emitting diode, visible light communication, high-bandwidth.

INTRODUCTION

Light-emitting diodes (LED) and μLEDs are suitable as light sources for visible light communications (VLC) owing to their advantages such as high bandwidth, low power, and being license-free.[1, 2] Hence, VLC-LEDs have been regarded as candidates for underwater wireless optical communication (UWOC), polymer optical fiber communication (POF), and light-fidelity (Li-Fi) networks applications. Green VLC-LEDs are particularly suitable for POF and UWOC applications because they produce only a small loss in the plastic fiber and seawater.[3, 4] The limitation of the 3-dB bandwidth for a VLC-LED device can be described by the following equation:

$$f_{-3dB} = \frac{\sqrt{3}}{2\pi\tau} = \frac{\sqrt{3}}{2\pi}\left(\frac{1}{\tau_r}+\frac{1}{\tau_{nr}}+\frac{1}{\tau_{RC}}\right), \qquad (1)$$

where τ is the lifetime of minority carrier, τ_r is the lifetime of radiative carrier, τ_{nr} is the lifetime of nonradiative carrier, and τ_{RC} is the RC time constant. In order to increase the f_{-3dB} bandwidth, it is preferable to shorten τ_r but not τ_{nr} because the carrier radiative lifetime has been established as the dominant factor limiting the f_{-3dB} bandwidth for LED devices with an active area close to micro-size or less.[5] In this situation, τ_r depends on the injected current density and is equal to $B^{-1} \times N$, where B and N denote the radiative coefficient and the carrier density, respectively. Thus, equation (1) takes the following form when a bimolecular recombination mechanism is assumed:[5]

$$f_{-3dB} = \frac{\sqrt{3}}{2\pi} \times \sqrt{\frac{BJ}{qd}}, \qquad (2)$$

where J denotes the injected current density, q stands for the elementary charge, and d is the active region thickness. Thus, equation (2) implies that higher 3-dB bandwidth can be realized by either increasing the operation current density, typically 5 to 10 kA/cm^2 for *c*-plane multiple quantum wells (MQWs) LEDs, or reducing the chip size to obtain a higher injected current density.[6] However, the commercially available GaN LEDs are usually grown on (0001) "polar" *c*-plane sapphire substrates, which can result in a strong quantum-confined Stark effect (QCSE) leading to the reduced efficiency (i.e., efficiency droop) under high injected current density conditions.[7] The QCSE is caused by the natural structure of GaN, a hexagonal crystal with wurtzite structure, where the existence of spontaneous polarization is due to the highest symmetry compatible.[8] Meanwhile, the MQWs sustain a large piezoelectric field due to the strain-induced polarization from the lattice mismatch between $In_xGa_{1-x}N$ and GaN. These internal polarization fields along the *c*-plane (*z*-axis) cause charge to accumulate at the heterojunction in MQWs, leading to the tilt of the energy band. The wave-function distribution of electrons and holes will be spatial separated, resulting in low carrier radiative recombination rate and low internal quantum efficiency. QCSE also leads to wavelength-shift and efficiency droop with increasing injected current density.[7, 9] Moreover, the QCSE in InGaN/GaN MQWs increases due to stronger polarization, larger lattice mismatch, high defect density, and stronger strain caused by the increase in indium (In) composition.[10] These phenomena in InGaN/GaN LEDs are the "green gap", limiting the development of green LEDs in the past decades.[11] The 3-dB bandwidth will be limited by QCSE when LEDs are utilized as optical transmitters for wireless communications.

One approach to overcome QCSE is to fabricate nonpolar structures on bulk GaN.[12] The polarization field can be completely eliminated when the growth orientation of the InGaN / GaN MQWs crystal plane lies perpendicular to the polar planes, e.g., along the (11-20) or the (1-100). However, such nonpolar *a*- or *m*-plane LEDs still emit a short wavelength of < 510 nm with low EQE, low output power due to low In incorporation, and poor epitaxial material quality.[13] The incorporation of In atoms into the semipolar plane has a much lower chemical potential requirement than that for both polar and nonpolar surfaces since the semipolar GaN surface has a lower repulsive interaction with the In atoms. Consequently, semipolar GaN crystals can accommodate a much higher In content, which is beneficial for long-wavelength MQWs in InGaN/GaN devices.[14] The most promising growth orientation for GaN-based long-wavelength devices is the semipolar plane. The applications of the semipolar (20-21) and (20-2-1) epitaxial structures have been proven to effectively suppress the effects of QCSE and bridge the green gap with a larger output power.[15-17] These superior devices can be achieved by free-standing GaN crystals that are prepared by either hydride vapor-phase epitaxy or ammonothermal epitaxial methods; however, they are still limited by the difficulty of obtaining GaN substrates. Until now, the GaN substrate is still an expensive material, commonly produced in small dimensions (e.g., 2-inch wafers). This problem limits the mass-production of semi-polar and nonpolar devices.

Since 2000, the progress of epitaxial processes for manufacturing nonpolar and semipolar structures can be divided on the basis of heteroepitaxy on substrates like sapphire, Si, SiC, and free-standing bulk GaN substrates.[18] Subsequently, epitaxial lateral overgrowth (ELOG) and orientation controlling epitaxy (OCE) are investigated for growing semipolar GaN with large-area by patterned substrates.[19, 20] Recent progress in heteroepitaxy has been achieved with selective area growth (SAG) of semipolar GaN from the inclined sidewall on striped sapphire or Si substratum.[21, 22] It is theoretically possible to access any orientation of GaN on large-size foreign substrates by SAG.[23] However, the semipolar and nonpolar GaN grown by OCE or SAG still produces stacking faults (SFs) with a certain magnitude of defect density while GaN coalesces to form a continuous film. In contrast to *c*-plane devices grown on sapphire, the initial development of semipolar and nonpolar GaN heteroepitaxy suffered from a high density of SFs consisting of basal-plane SFs (BSFs) and prismatic SFs (PSFs) associated with BSFs, which lead to a high defect density in the epitaxial layer.[24] In the case of *c*-plane-grown GaN, the SFs cannot extend to the surface, and thus their influence can be ignored. However, the SF planes are parallel or inclined to the growth orientation of nonpolar or semipolar GaN. Consequently, SFs can cross over the upper layers and extend to the active region. Both BSFs and PSFs are supposed to affect the property of the semipolar GaN device. Most defects, which grow along the underlying epitaxial layer, also affect the number of defects in the active region. The existing defects in the active region of a GaN-based optical-electrical device act as non-radiative recombination centers to capture electrons via phonon emission. An electron captured by the defects can then recombine with a valence band hole, again accompanied by the emission of phonons. Thus, an electron falls from the conduction band to the valence band via at least two transitions; however, most of the energy released is dissipated as heat. This non-radiative recombination process also called the Shockley-Read-Hall (SRH) recombination or trap-assisted recombination. This is also related to the droop effect of the LEDs.[25] In order to improve the epitaxial quality and achieve high-performance devices, it is important to further eliminate SFs. In our previous study, we investigated a SAG technique utilizing a Germanium-doped (Ge-doped) process to realize SF-free semipolar (20-21) LEDs on large scale (4-inch) patterned sapphire substrates.[24] The performance of this device was comparable to the free-standing semipolar device with an emission wavelength of 455 nm, a spectral linewidth of 22 nm, and a maximum EQE of 24%. These results indicate that the semipolar GaN devices has the potential for developing high-speed VLC applications owing to the elimination of QCSE and improved material quality.

In this work, long-wavelength (initial wavelength 540 nm) InGaN/GaN VLC-LEDs with a high 3-dB bandwidth were realized using semipolar epitaxy and μLED structure. The superior optical-electrical properties of this work were developed by an advanced epitaxial process and chip structure design. For instance, atomic layer deposition (ALD) was introduced to eliminate the surface defects caused by the size effect and reduce the leakage current. As a result, the semipolar (20-21) μLED achieves the highest-ever 3-dB bandwidth in long-wavelength InGaN/GaN LED devices, to the best of our knowledge.

EXPERIMENTS

The epitaxial process of semipolar (20-21) GaN on a (22-43) PSS is carried out through a low-pressure metalorganic chemical vapor deposition (MOCVD). The offset angle of the (22-43) sapphire was adjusted to fit the (20-21) GaN surface precisely with the substrate surface. The angle between (20-21) GaN and *c*-plane GaN is 75.09°, while the angle between (22-43) sapphire and *c*-plane sapphire is 74.64°. Hence, the final offset angle is 0.45°. The (22-43) PSS was prepared using photolithography and inductively coupled plasma reactive-ion etching (ICP-RIE) process. The depth and width of the grooves and terraces for the linear trenches are 1 μm, 3 μm, and 6 μm, respectively. Beyond the selected *c*-plane sapphire sidewall, a self-aligned technique of angled evaporation was used to deposit silicon oxide on the surfaces of the entire substrate. After preparing the substrates, semipolar (20-21) GaN was grown. In the early stage of epitaxy, Ge-doping was used to avoid the formation of SFs during GaN coalescence. The detailed principle of elimination for SFs can be found in our previous work.[24] An 8-μm-thick un-doped GaN was grown after the adjacent Ge-doped GaN stripes coalesced, resulting in a bulk layer approximately 10 μm thick. The wafer was then removed from the MOCVD set-up and planarized using the chemical-mechanical planarization process to achieve a smooth surface for growing InGaN/GaN LED on (20-21) GaN templates. The LED structure consisted of a 1.5-μm-thick *n*-type GaN, followed by 3 pairs of InGaN/GaN MQWs as the active region and a 100-nm-thick *p*-type GaN layer.

The μLED process starts with the deposition of a 200-nm-thick indium tin oxide (ITO) layer, followed by using HCl solution and ICP-RIE for etching the ITO film and the

1-μm-depth mesa, respectively. The sample was then annealed at 450°C under atmospheric ambiance via a rapid thermal process to form a *p*-type ohmic contact. Subsequently, Ti/Al/Ti/Au with a thickness of 20/150/10/100 nm was deposited as the electrodes. ALD technology was introduced for growing the passivation layer of the VLC μLED device. The passivation layer of aluminum oxide (Al_2O_3) was grown in an argon (Ar) environment at 300°C by applying the cycle for trimethylaluminum (TMA) and H_2O, with Ar purging. After depositing a 30-nm-thick passivation layer, 200-nm-thick SiO_2 layer was grown by plasma enhanced chemical vapor deposition (PECVD) and the via hole process by ICP-RIE. Ti/Al/Ni/Au was deposited again as the pad metal and sidewall reflector. Finally, the rear side of the wafer was deposited with a distributed Bragg reflector (DBR).

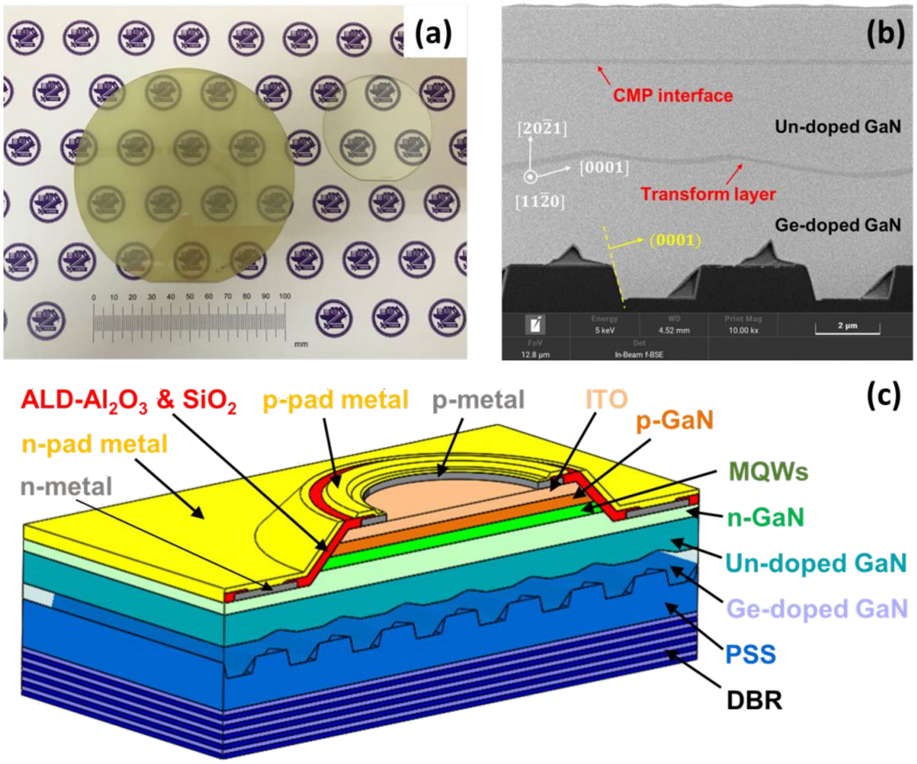

Fig. 1. (a) A 4-inch semipolar (20-21) green LED epitaxial wafer and a 2-inch commercially available *c*-plane InGaN/GaN LED wafer with its rear side polished; (b) SEM image of semipolar LED with the cross-sectional view; (c) schematic diagram of semipolar (20-21) μLED structures.

RESULTS AND DISCUSSION

In Fig. 1(a), the National Chiao Tung University logo is visible clearly as a reference through a 4-inch semipolar (20-21) green LED epitaxial wafer and 2-inch *c*-plane epitaxial wafer (rear side polished). The high degree of transparency for both wafers reveals the uniformity and low defect density. Large-area, low-cost epitaxial technology helps increase the application potential of semipolar LEDs. The SEM image (Fig. 1(b)) shows the complete LED epitaxial layer and labels the crystalline planes of GaN with a surface normal direction toward (20-21) GaN. In a previous study, Ge doping was found that can change the growth rate of N-polar (000-1) facets and decelerate the growth rate of (101-1), resulting in the elimination of SFs generated in the (000-1) facets. This method significantly improves the quality of heteroepitaxial semipolar GaN and achieves XRD rocking curves of the on-axis (20-21) plane with the full width at half maximum (FWHM) of 192 and 217 arc sec to the rocking axis perpendicular or parallel to the patterned stripes, respectively.[24], Comparable with those of *c*-plane epitaxy, these values suggest the bulk GaN layer with a high crystal quality. Further, in Fig. 1(c), the μLED device has been optimized by various designs to achieve high performance in VLC properties. The core technologies in the concept of this device are as follows:

(i) The electrode has been minimized to reduce the capacitance in order to reach a small RC time constant.

(ii) The circular active area and the electrode used to improve the spreading of current and enhance the electrical performance.

(iii) An Al_2O_3 layer deposited by the atomic layer deposition (ALD) was utilized to erase the influence of sidewall defects from the etching process.

(iv) The DBR on the rear side was deposited by the evaporation machine and consisted of multiple pairs of SiO_2/TiO_2. The designed thickness of SiO_2/TiO_2 layer in each pair was 72 nm and 50 nm, respectively.

Some previous studies have stated that the influence of sidewall defects increase as the chip size decreases.[26, 27] In particular, when the LED device achieves a micrometer scale, traditional passivation methods such as the PECVD process, is no longer useful towing to the large leakage current of the μLED device. ALD dielectric thin films have been regarded as an effective passivation technique in the μLED area.[28] The rear DBR can achieve a reflectivity of 90% for wavelengths between 460 to 550 nm with a number of 10.5 pairs in this work and helps enhance the output power.[29]

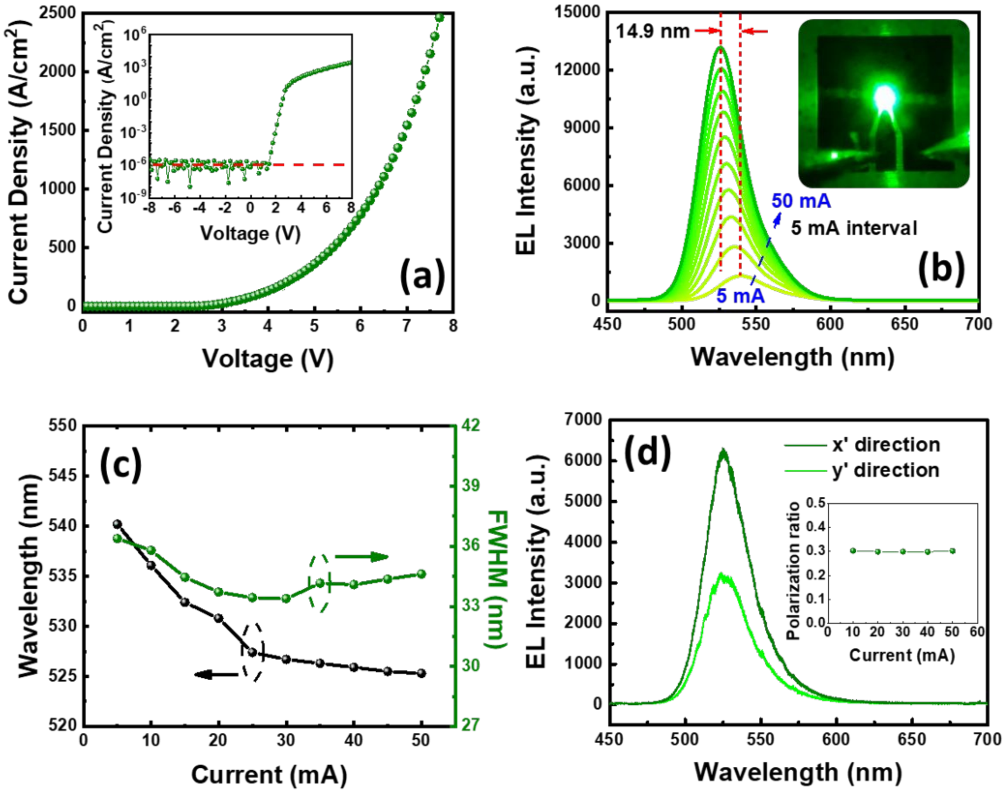

Fig. 2. (a) J-V curve of semipolar μLEDs; (b) EL spectra at different currents, and an image of lighting from device; (c) wavelength shift and FWHM as a function of currents; (d) EL spectra at 50 mA along the x'- and y'-directions, and the polarization ratio at different currents.

Figure 2 summarizes the optical and electrical performance of semipolar (20-21) μLEDs. The current density versus voltage (J-V) curve is shown in Fig. 2(a). The current density was normalized by the active region area, and the maximum applied current of 50 mA corresponds to 2546 A/cm^2 in this study. The 2.2 V turn-on voltage is regarded as a reasonable performance of the green μLED. This result indicates good material properties and device processes. It's worth noting that this device shows a relatively larger resistance which may cause by the inverse polarization due to the additional energy barriers in MQWs or the poor ohmic contact in the *p*-type region.[30] But the large resistance cannot significantly affect the 3-dB bandwidth of the device because of the extremely small capacitance for microscale LEDs.[5] The inset in Fig. 2(a) demonstrates a J–V curve at the reverse voltage, which is used to observe the leakage current. The low leakage current density (about 10^{-6} A/cm^2) achieved under -8 V can be attributed to the ALD passivation process and the low defect density in semipolar (20-21) GaN. Several studies report the proportional relationship between the leakage current and the defect density.[28, 31, 32] Moreover, sidewall defects and surface recombination dominate the generation of leakage currents as the chip size shrinks in GaN-based LED devices. These surface states are mainly caused by the sidewall damage during the dry etching. J. Kou *et al.* also demonstrated that the injection capability for carriers was severely affected by sidewall defects, reducing the device performance.[26] Wang *et al.* reported a comparison of ALD and PECVD passivation for μLED devices.[28] The results show that ALD has a marked passivating effect while PECVD fails to confine the leakage current for μLEDs smaller than the chip size specified. The above description illustrates the importance of the ALD passivation process in this study and μLED related applications. In Fig. 2(b) and (c) demonstrate the electroluminescence (EL) emission spectra and the spectral properties for the semipolar (20-21) μLED with increasing injected current (5 mA as an interval), respectively. The inset in Fig. 2(b) illustrates a photograph of μLED operating at 10 mA. The μLED device illustrates a peak-wavelength shift of 14.9 nm and becomes stabilized from 5 to 50 mA. This wavelength shift can be considered a good performance compared to common *c*-plane devices. It originates in the reduced polarization-related electric field, and flattens the energy bandgap of the quantum wells, implying an improved QCSE. Meanwhile, the FWHM of the emission spectra is only 3 nm change (including the maximum change) from 5 to 50 mA, which indicates low defect density and good uniformity in the distribution of In atoms.

Furthermore, the higher polarization ratio is an advantage of semipolar LEDs compared with *c*-plane-grown

LEDs. Fig. 2(d) illustrates the EL spectra of the semipolar μLED at 50 mA with the polarizer aligned along the [1-210] and [10-1-4] directions, which are defined as the x'- and y'-directions that correspond to the maximum and minimum intensities through the polarizer, respectively. The following equation can be used to determine the optical polarization ratio:

$$\rho = \frac{I_{x'} - I_{y'}}{I_{x'} + I_{y'}}, \tag{3}$$

where $I_{x'}$ and $I_{y'}$ denote the integrated intensities of EL spectra in the x'- and y'-directions, respectively. The polarization ratio is 0.3 for the EL spectra at 50 mA, and this value is consistent with previous studies.[33, 34] In InGaN-based semipolar LEDs, a longer wavelength (i.e., higher In content) exhibits a larger polarization ratio because of the optical transition between the conduction band and the highest valence band .[33] The inset in Fig. 2(d) illustrates the polarization ratio with increasing injected currents. The plotted data illustrate that the polarization ratio is independent of the injected current. These results suggest that the InGaN layers were homogeneous in the MQWs.[35] Such polarization characteristics can be applied to polarization-division multiplexing to increase the data transmission rate and introduce another degree of freedom that can multiply the transmission capacity, compared to the traditional VLC works.[36]

Figure 3 presents the time-resolved photoluminescence (TRPL) measurement of the semipolar (20-21) μLED and commercial *c*-plane green μLED (as a reference, produced by Epistar Inc.) with PL peak wavelengths of 534 and 529 nm, respectively. TRPL measurements were conducted at a low power of 20 μW at room temperature to ensure that excitonic recombination dominated the recombination process. The carrier decline dynamic parameter of the InGaN / GaN LED system can be derived from a double-exponential fit representing a decline in PL of two components by relaxing localized excitons, and the excitonic relaxation of free carriers and localized states, respectively. The normalized TRPL trace [*I(t)*] can be used to calculate the minority carrier lifetime τ as follows:[37]

$$I(t) = \alpha_1 \exp(-\frac{t}{\tau_1}) + \alpha_2 \exp(-\frac{t}{\tau_2}), \tag{4}$$

$$R_i = \frac{\alpha_i}{\sum_{i=1}^{2} \alpha_i}, \tag{5}$$

where α_1 and τ_1 (or α_2 and τ_2) define as the fast or slow decay components corresponding to localized excitons and excitonic relaxation of free carriers and localized states, respectively, and R_i is the relative ratio factor. Using the parameter extracted from fitting results (as the table shown in Fig. 3), the minority carrier lifetime τ of each sample found to be 2.65 ns and 9.00 ns, respectively. The shorter lifetime of semipolar samples are due to the weak polarized field and flat energy gap distribution which lead to larger electron-hole wave-function overlap reducing the τ_r, and the smaller In fluctuations that reduce the τ_{nr} in a comparison between the semipolar and *c*-plane samples[12] Faster carrier recombination corresponds to the higher 3-dB bandwidth in similar LEDs. Further, Zhao *et al.* revealed that faster carrier transport in semipolar devices also contributes to the weaker phase-space filling effect which was determined for the low-droop phenomenon in semipolar LEDs because of small QCSE and short carrier lifetimes using the consistency between theoretical and experimental results.[38] The aforementioned advantages imply that a semipolar LED is capable of simultaneously achieving high modulation speed and maintaining high efficiency with increasing injected current owing to low droop performance.

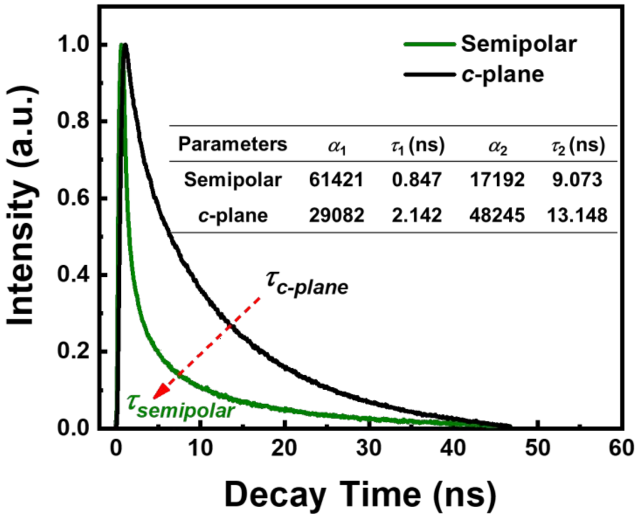

Parameters	α_1	τ_1 (ns)	α_2	τ_2 (ns)
Semipolar	61421	0.847	17192	9.073
c-plane	29082	2.142	48245	13.148

Fig. 3. TRPL curves of semipolar (20-21) μLED and *c*-plane μLED.

Figure 4 shows the VLC performance of the 50 μm diameter device as the current increases. As shown in Fig. 4(a), the frequency response measurement was carried out using a vector network analyzer (VNA; HP 8720ES). The alternating current from the VNA was added to a direct current bias via a bias tee and then applied to the μLED device which was probed by a high-speed microprobe (ACP40-GS-250). A plastic optical fiber was used to collect the light of the semipolar μLED, coupled to a photodetector (SPA-3) and then send the converted electrical signal to the VNA. In Fig. 4(b), the 3-dB bandwidth increased with the current density because of the built-in electric field screening and decreased carrier lifetime due to the higher injected carrier density in the active region. As a result, the highest 3-dB bandwidth which is up to 756 MHz was realized by an injected current of 40 mA. Moreover, the 3-dB bandwidth is proportional to the increasing current density, as shown in the inset of Fig. 4(b). This suggests that the RC delay did not restrict the 3-dB bandwidth under these operating conditions, leading to the conclusion that the 3-dB bandwidth for micro-scale devices is not constrained by RC but the recombination lifetime. The data rate measurement system was set up to show the actual data transmission property, as shown in Fig. 4(c). The back-to-back non-return-to-zero on-off keying (NRZ-OOK) 2^7-1 pseudo-random bit sequence (PRBS-7) was generated by Anritsu MP1800A and the results of eye diagrams were recorded by the Tektronix DPO 7354C oscilloscope. Due to the impressive performance of the 3-dB bandwidth, the eye diagrams of the semipolar µLED were clear and open at both 1.0 and 1.5 Gb/s in Fig. 4(d). However, the eye area was no longer clear when the data rate toward to 2 Gb/s due to the relatively low signal-to-noise ratio. It is expected to obtain a higher data rate through high-level modulation methods in the future.

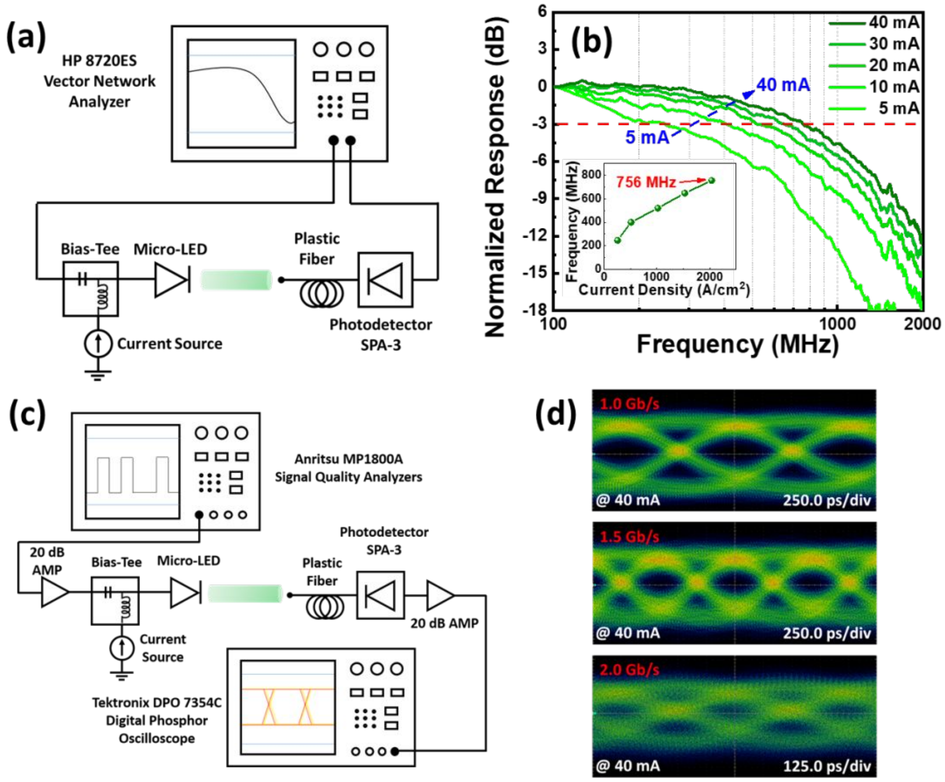

Fig. 4. For the 50-µm semipolar (20-21) µLED, (a) Schematic diagrams with (b) results for the frequency response measurement, and (c) schematic diagrams with (d) eye diagrams for the data rate measurement.

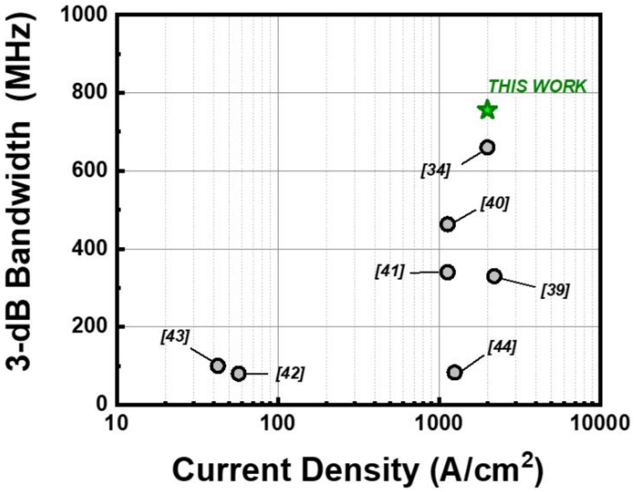

Fig. 5. Benchmark of 3-dB bandwidth for long-wavelength light-emitting diodes with applied current density.

Figure 5 shows the benchmark of the 3-dB bandwidth versus the current density for the long-wavelength (> 500 nm) InGaN LED devices with different achievements. In 2008, Lai *et al*. illustrated a *c*-plane green (peak wavelength 510 nm) LED and achieved a bandwidth of 330 MHz under a 2.2 kA/cm² injected current density.[39] Wu *et al.* demonstrated a bandwidth close to 463 MHz for the *c*-plane (peak wavelength 500 nm) LED with a 75-µm aperture diameter incorporating the improvement of a ring-shaped electrode, and achieved a high data rate in 2014 and 2018, respectively.[40, 41] J. Li *et al*. demonstrated a surface plasma coupled method to enhance the 3-dB bandwidth for the *c*-plane green (peak wavelength 540 nm) LEDs that achieve 80 MHz frequency under 100 mA using a normal chip 418 µm in diameter.[42] In 2016, Corbett et al. reported green (peak wavelength of ~550 nm) LED devices grown on semipolar (11-22) GaN templates and showing a 100 MHz bandwidth under 30 mA.[43] In 2018, Mei *et al.* introduced a perovskite quantum dots converted white LED with 83 MHz bandwidth, which provides another approach to realize VLC application.[44] In 2020, Khoury *et al*. demonstrated the first monolithic white semipolar (20-21) LEDs and achieved a 660 MHz bandwidth with a chip diameter of 20 µm.[34] To the best of our knowledge, this study shows the highest 3-dB bandwidth of 756 MHz (at 2.0 kA/cm²) achieved by long-wavelength InGaN LED devices. Based on our previous results for semipolar (20-21) LED technology, this device has been improved in terms of the Ge-doped epitaxial process, chip structure design, and ALD passivation.

CONCLUSION

In conclusion, a high 3-dB bandwidth semipolar (20-21) long-wavelength InGaN/GaN μLED has been demonstrated. The SF-free semipolar LED is successfully fabricated, and its superior optical-electrical performance indicates good epitaxial quality through the improvement of the Ge-doped SAG process. By introducing chip structure optimization and ALD passivation, this device shows the highest 3-dB bandwidth of 756 MHz at 2.0 kA/cm^2 with a 525 nm peak wavelength and high polarized properties. The breakthrough in this 3-dB bandwidth allows semipolar LEDs an attractive part to realize VLC at high speed.

AUTHOR INFORMATION

Corresponding Author

Tingzhu Wu - Department of Electronic Science, School of Electronic Science and Engineering, Xiamen University, Xiamen 361005, China; Email: wutingzhu@xmu.edu.cn

Hao-Chung Kuo - Department of Photonics & Graduate Institute of Elecro-Optical Engineering, College of Electrical and Computer Engineering, National Chiao Tung University, Hsinchu 30010, Taiwan; Email: hckuo@faculty.nctu.edu.tw

Authors

Sung-Wen Huang Chen - Department of Photonics & Graduate Institute of Elecro-Optical Engineering, College of Electrical and Computer Engineering, National Chiao Tung University, Hsinchu 30010, Taiwan

Yu-Ming Huang - Institute of Photonic System, National Chiao-Tung University, Tainan 71150, Taiwan

Yun-Han Chang - Department of Photonics & Graduate Institute of Elecro-Optical Engineering, College of Electrical and Computer Engineering, National Chiao Tung University, Hsinchu 30010, Taiwan

Yue Lin - Department of Electronic Science, School of Electronic Science and Engineering, Xiamen University, Xiamen 361005, China

Fang-Jyun Liou - Department of Photonics & Graduate Institute of Elecro-Optical Engineering, College of Electrical and Computer Engineering, National Chiao Tung University, Hsinchu 30010, Taiwan

Yu-Chien Hsu - Department of Photonics & Graduate Institute of Elecro-Optical Engineering, College of Electrical and Computer Engineering, National Chiao Tung University, Hsinchu 30010, Taiwan

Jie Song - Saphlux Inc, Branford, Connecticut 06405, United States

Joowon Choi - Saphlux Inc, Branford, Connecticut 06405, United States

Chi-Wai Chow - Department of Photonics & Graduate Institute of Elecro-Optical Engineering, College of Electrical and Computer Engineering, National Chiao Tung University, Hsinchu 30010, Taiwan

Chien-Chung Lin - Institute of Photonic System, National Chiao-Tung University, Tainan 71150, Taiwan

Ray-Hua Horng - Institute of Electronics, National Chiao Tung University, Hsinchu 30010, Taiwan

Zhong Chen - Department of Electronic Science, School of Electronic Science and Engineering, Xiamen University, Xiamen 361005, China

Jung Han - Department of Electrical Engineering, Yale University, New Haven, Connecticut 06520, United States

Notes

The authors declare no competing financial interest

FUNDING SOURCES

Ministry of Science and Technology, Taiwan (MOST) (MOST 107-2221-E-009-113-MY3, 108-2221-E-009-113-MY3). National Natural Science Foundation of China (11904302). Major Science and Technology Project of Xiamen, China (3502Z20191015).

ACKNOWLEDGMENT

The authors would like to thank Prof. Nakamura and Prof. Steven Denbaars of UCSB, Prof. Gong-Ru Lin and Dr. Chun-Jung Lin of National Taiwan University for the helpful discussion.

REFERENCES

(1) Hsu, C.-W.; Chow, C.-W.; Lu, I. C.; Liu, Y.-L.; Yeh, C.-H.; Liu, Y., High speed imaging 3 x 3 MIMO phosphor white-light LED based visible light communication system. *IEEE Photonics J.* **2016,** *8* (6), 7907406.

(2) Wu, T.; Sher, C.-W.; Lin, Y.; Lee, C.-F.; Liang, S.; Lu, Y.; Chen, S.-W. H.; Guo, W.; Kuo, H.-C.; Chen, Z., Mini-LED and micro-LED: Promising candidates for the next generation display technology. *Appl. Sci.* **2018,** *8* (9), 1557.

(3) McKendry, J. J. D.; Green, R. P.; Kelly, A. E.; Gong, Z.; Guilhabert, B.; Massoubre, D.; Gu, E.; Dawson, M. D., High-speed visible light communications using individual pixels in a micro light-emitting diode array. *IEEE Photonic. Tech. L.* **2010,** *22* (18), 1346-1348.

(4) Liu, X.; Yi, S.; Zhou, X.; Fang, Z.; Qiu, Z.-J.; Hu, L.; Cong, C.; Zheng, L.; Liu, R.; Tian, P., 34.5 m underwater optical wireless communication with 2.70 Gbps data rate based on a green laser diode with NRZ-OOK modulation. *Opt. Express* **2017,** *25* (22), 27937-27947.

(5) Haemmer, M.; Roycroft, B.; Akhter, M.; Dinh, D. V.; Quan, Z.; Zhao, J.; Parbrook, P. J.; Corbett, B., Size-dependent bandwidth of semipolar (11(2)over-bar2) light-emitting-diodes. *IEEE Photonic. Tech. L.* **2018,** *30* (5), 439-442.

(6) Monavarian, M.; Rashidi, A.; Aragon, A. A.; Oh, S. H.; Rishinaramangalam, A. K.; DenBaars, S. P.; Feezell, D., Impact of crystal orientation on the modulation bandwidth of InGaN/GaN light-emitting diodes. *Appl. Phys. Lett.* **2018,** *112* (4), 041104.

(7) Piprek, J., Efficiency droop in nitride-based light-emitting diodes. *Phys. Status Solidi A* **2010,** *207* (10), 2217-2225.

(8) Bernardini, F.; Fiorentini, V.; Vanderbilt, D., Spontaneous polarization and piezoelectric constants of III-V nitrides. *Phys. Rev. B* **1997,** *56* (16), 10024-10027.

(9) Takeuchi, T.; Sota, S.; Katsuragawa, M.; Komori, M.; Takeuchi, H.; Amano, H.; Akasaki, I., Quantum-confined stark effect due to piezoelectric fields in GaInN strained quantum wells. *Jpn. J. Appl. Phys.* **1997,** *36* (4A), L382-L385.

(10) Zhao, Y.; Yan, Q.; Huang, C.-Y.; Huang, S.-C.; Hsu, P. S.; Tanaka, S.; Pan, C.-C.; Kawaguchi, Y.; Fujito, K.; Van de Walle, C. G.; Speck, J. S.; DenBaars, S. P.; Nakamura, S.; Feezell, D., Indium incorporation and emission properties of nonpolar and semipolar InGaN quantum wells. *Appl. Phys. Lett.* **2012,** *100* (20), 201108.

(11) Jiang, Y.; Li, Y.; Li, Y.; Deng, Z.; Lu, T.; Ma, Z.; Zuo, P.; Dai, L.; Wang, L.; Jia, H.; Wang, W.; Zhou, J.; Liu, W.; Chen, H., Realization of high-luminous-efficiency InGaN light-emitting diodes in the "green gap" range. *Sci. Rep.* **2015,** *5*, 10883.

(12) Zhao, Y.; Fu, H.; Wang, G. T.; Nakamura, S., Toward ultimate efficiency: progress and prospects on planar and 3D nanostructured

nonpolar and semipolar InGaN light-emitting diodes. *Adv. Opt. Photonics* **2018,** *10* (1), 246-308.

(13) Mukai, T.; Yamada, M.; Nakamura, S., Characteristics of InGaN-based UV/blue/green/amber/red light-emitting diodes. *Jpn. J. Appl. Phys.* **1999,** *38* (7A), 3976-3981.

(14) Johar, M. A.; Song, H.-G.; Waseem, A.; Kang, J.-H.; Ha, J.-S.; Cho, Y.-H.; Ryu, S.-W., Ultrafast carrier dynamics of conformally grown semi-polar (1122) GaN/InGaN multiple quantum well co-axial nanowires on m-axial GaN core nanowires. *Nanoscale* **2019,** *11* (22), 10932-10943.

(15) Zhao, Y.; Tanaka, S.; Pan, C.-C.; Fujito, K.; Feezell, D.; Speck, J. S.; DenBaars, S. P.; Nakamura, S., High-power blue-violet semipolar (20(2)over-bar(1)over-bar) InGaN/GaN light-emitting diodes with low efficiency droop at 200 A/cm^2. *Appl. Phys. Express* **2011,** *4* (8), 082104.

(16) Feezell, D. F.; Speck, J. S.; DenBaars, S. P.; Nakamura, S., Semipolar (20(2)over-bar(1)over-bar) InGaN/GaN light-emitting diodes for high-efficiency solid-state lighting. *J. Disp. Technol.* **2013,** *9* (4), 190-198.

(17) Chen, S.-W. H.; Huang, Y.-M.; Singh, K. J.; Hsu, Y.-C.; Liou, F.-J.; Song, J.; Choi, J.; Lee, P.-T.; Lin, C.-C.; Chen, Z.; Han, J.; Wu, T.; Kuo, H.-C., Full-color micro-LED display with high color stability using semipolar (20-21) InGaN LED and quantum-dot photoresist. *Photonics Res.* **2020,** *8* (5), 630-636.

(18) Waltereit, P.; Brandt, O.; Trampert, A.; Grahn, H. T.; Menniger, J.; Ramsteiner, M.; Reiche, M.; Ploog, K. H., Nitride semiconductors free of electrostatic fields for efficient white light-emitting diodes. *Nature* **2000,** *406* (6798), 865-868.

(19) Guehne, T.; Bougrioua, Z.; Lauegt, S.; Nemoz, M.; Vennegues, P.; Vinter, B.; Leroux, M., Band-edge photoluminescence and reflectivity of nonpolar (11(2)over-bar0) and semipolar (11(2)over-bar2) GaN formed by epitaxial lateral overgrowth on sapphire. *Phys. Rev. B* **2008,** *77* (7), 075308.

(20) Leung, B.; Sun, Q.; Yerino, C. D.; Han, J.; Coltrin, M. E., Using the kinetic Wulff plot to design and control nonpolar and semipolar GaN heteroepitaxy. *Semicond. Sci. Technol.* **2012,** *27* (2), 024005.

(21) Sawaki, N.; Honda, Y.; Hikosaka, T.; Tanaka, S.; Yamaguchi, M.; Koide, N.; Tomita, K., Selective growth and impurity incorporation in semipolar GaN grown on Si substrate. In *Gallium Nitride Materials and Devices V*, Chyi, J. I.; Nanishi, Y.; Morkoc, H.; Litton, C. W.; Piprek, J.; Yoon, E., Eds. 2010; Vol. 7602.

(22) Scholz, F.; Meisch, T.; Caliebe, M.; Schoerner, S.; Thonke, K.; Kirste, L.; Bauer, S.; Lazarev, S.; Baumbach, T., Growth and doping of semipolar GaN grown on patterned sapphire substrates. *J. Cryst. Growth* **2014,** *405*, 97-101.

(23) Leung, B.; Wang, D.; Kuo, Y.-S.; Han, J., Complete orientational access for semipolar GaN devices on sapphire. *Phys. Status Solidi B* **2016,** *253* (1), 23-35.

(24) Song, J.; Choi, J.; Zhang, C.; Deng, Z.; Xie, Y.; Han, J., Elimination of stacking faults in semipolar GaN and light-emitting diodes grown on sapphire. *ACS Appl. Mater. Interfaces* **2019,** *11* (36), 33140-33146.

(25) Olivier, F.; Daami, A.; Licitra, C.; Templier, F., Shockley-Read-Hall and Auger non-radiative recombination in GaN based LEDs: A size effect study. *Appl. Phys. Lett.* **2017,** *111* (2), 022104.

(26) Kou, J.; Shen, C.-C.; Shao, H.; Che, J.; Hou, X.; Chu, C.; Tian, K.; Zhang, Y.; Zhang, Z.-H.; Kuo, H.-C., Impact of the surface recombination on InGaN/GaN-based blue micro-light emitting diodes. *Opt. Express* **2019,** *27* (12), A643-A653.

(27) Yang, W.; Zhang, S.; McKendry, J. J. D.; Herrnsdorf, J.; Tian, P.; Gong, Z.; Ji, Q.; Watson, I. M.; Gu, E.; Dawson, M. D.; Feng, L.; Wang, C.; Hu, X., Size-dependent capacitance study on InGaN-based micro-light-emitting diodes. *J. Appl. Phys.* **2014,** *116* (4), 044512.

(28) Wong, M. S.; Hwang, D.; Alhassan, A. I.; Lee, C.; Ley, R.; Nakamura, S.; Denbaars, S. P., High efficiency of III-nitride micro-light-emitting diodes by sidewall passivation using atomic layer deposition. *Opt. Express* **2018,** *26* (16), 21324-21331.

(29) Chang, S. J.; Shen, C. F.; Hsieh, M. H.; Kuo, C. T.; Ko, T. K.; Chen, W. S.; Shei, S. C., Nitride-based LEDs with a hybrid Al mirror +TiO_2/SiO_2 DBR backside reflector. *J. Lightwave Technol.* **2008,** *26* (17-20), 3131-3136.

(30) Kawaguchi, Y.; Huang, C.-Y.; Wu, Y.-R.; Yan, Q.; Pan, C.-C.; Zhao, Y.; Tanaka, S.; Fujito, K.; Feezell, D.; Van de Walle, C. G.; DenBaars, S. P.; Nakamura, S., Influence of polarity on carrier transport in semipolar (20(21)over-bar) and (20(2)over-bar1) multiple-quantum-well light-emitting diodes. *Appl. Phys. Lett.* **2012,** *100* (23), 231110.

(31) Chang, Y.-A.; Chang, J.-Y.; Kuo, Y.-T.; Kuo, Y.-K., Investigation of green InGaN light-emitting diodes with asymmetric AlGaN composition-graded barriers and without an electron blocking layer. *Appl. Phys. Lett.* **2012,** *100* (25), 251102.

(32) Cao, X. A.; Teetsov, J. A.; Shahedipour-Sandvik, F.; Arthur, S. D., Microstructural origin of leakage current in GaN/InGaN light-emitting diodes. *J. Cryst. Growth* **2004,** *264*, 172-177.

(33) Kyono, T.; Yoshizumi, Y.; Enya, Y.; Adachi, M.; Tokuyama, S.; Ueno, M.; Katayama, K.; Nakamura, T., Optical polarization characteristics of InGaN quantum wells for green laser diodes on semi-polar {20(2)over-bar1} GaN substrates. *Appl. Phys. Express* **2010,** *3* (1), 011003.

(34) Khoury, M.; Li, H.; Li, P.; Chow, Y. C.; Bonef, B.; Zhang, H.; Wong, M. S.; Pinna, S.; Song, J.; Choi, J.; Speck, J. S.; Nakamura, S.; DenBaars, S. P., Polarized monolithic white semipolar (20-21) InGaN light-emitting diodes grown on high quality (20-21) GaN/sapphire templates and its application to visible light communication. *Nano Energy* **2020,** *67*, 104236.

(35) Chung, R. B.; Lin, Y.-D.; Koslow, I.; Pfaff, N.; Ohta, H.; Ha, J.; DenBaars, S. P.; Nakamura, S., Electroluminescence characterization of (20(2)over-bar1) InGaN/GaN light emitting diodes with various wavelengths. *Jpn. J. Appl. Phys.* **2010,** *49* (7), 070203.

(36) Hsu, C.-W.; Yeh, C.-H.; Chow, C.-W., Using adaptive equalization and polarization-multiplexing technology for gigabit-per-second phosphor-LED wireless visible light communication. *Opt. Laser Technol.* **2018,** *104*, 206-209.

(37) Huang Chen, S.-W.; Shen, C.-C.; Wu, T.; Liao, Z.-Y.; Chen, L.-F.; Zhou, J.-R.; Lee, C.-F.; Lin, C.-H.; Lin, C.-C.; Sher, C.-W.; Lee, P.-T.; Tzou, A.-J.; Chen, Z.; Kuo, H.-C., Full-color monolithic hybrid quantum dot nanoring micro light-emitting diodes with improved efficiency using atomic layer deposition and nonradiative resonant energy transfer. *Photonics Res.* **2019,** *7* (4), 416-422.

(38) Fu, H.; Lu, Z.; Zhao, X.-H.; Zhang, Y.-H.; DenBaars, S. P.; Nakamura, S.; Zhao, Y., Study of low-efficiency droop in semipolar (20(2)over-bar(1)over-bar) InGaN light-emitting diodes by time-resolved photoluminescence. *J. Disp. Technol.* **2016,** *12* (7), 736-741.

(39) Shi, J. W.; Sheu, J. K.; Chen, C. H.; Lin, G. R.; Lai, W. C., High-speed GaN-based green light-emitting diodes with partially n-doped active layers and current-confined apertures. *IEEE Electr. Device L.* **2008,** *29* (2), 158-160.

(40) Liao, C.-L.; Ho, C.-L.; Chang, Y.-F.; Wu, C.-H.; Wu, M.-C., High-speed light-emitting diodes emitting at 500 nm with 463-MHz modulation bandwidth. *IEEE Electr. Device L.* **2014,** *35* (5), 563-565.

(41) Chen, C.-J.; Yan, J.-H.; Chen, D.-H.; Lin, K.-H.; Feng, K.-M.; Wu, M.-C. A 520-nm green GaN LED with high bandwidth and low current density for gigabits OFDM data communication, In *2018 Optical Fiber Communications Conference and Exposition*, Optical Society of America, 2018.

(42) Li, J.; Gou, P.; Chi, N.; Ou, H. Enhanced emission and modulation properties of localized surface plasma coupled GaN-based green light-emitting diodes, In *2018 Optical Fiber Communications Conference and Exposition*, Optical Society of America, 2018.

(43) Corbett, B.; Quan, Z.; Dinh, D. V.; Kozlowski, G.; O'Mahony, D.; Akhter, M.; Schulz, S.; Parbrook, P.; Maaskant, P.; Caliebe, M.; Hocker, M.; Thonke, K.; Scholz, F.; Pristovsek, M.; Han, Y.; Humphreys, C. J.; Brunner, F.; Weyers, M.; Meyer, T. M.; Lymperakis, L., Development of semipolar (11-22) LEDs on GaN templates. In *Light-Emitting Diodes: Materials, Devices, and Applications for Solid State Lighting Xx*, Jeon, H.; Tu, L. W.; Krames, M. R.; Strassburg, M., Eds. 2016; Vol. 9768.

(44) Mei, S.; Liu, X.; Zhang, W.; Liu, R.; Zheng, L.; Guo, R.; Tian, P., A high-bandwidth white-light system combining a micro-LED with perovskite quantum dots for visible light communication. *ACS Appl. Mater. Interfaces* **2018,** *10*, 5641-5648.

For Table of Contents Use Only

Manuscript title:

High-bandwidth green semipolar (20-21) InGaN/GaN micro light-emitting diodes for visible light communication

Names of authors:

Sung-Wen Huang Chen, Yu-Ming Huang, Yun-Han Chang, Yue Lin, Fang-Jyun Liou, Yu-Chien Hsu, Jie Song, Joowon Choi, Chi-Wai Chow, Chien-Chung Lin, Ray-Hua Horng, Zhong Chen, Jung Han, Tingzhu Wu*, and Hao-Chung Kuo*

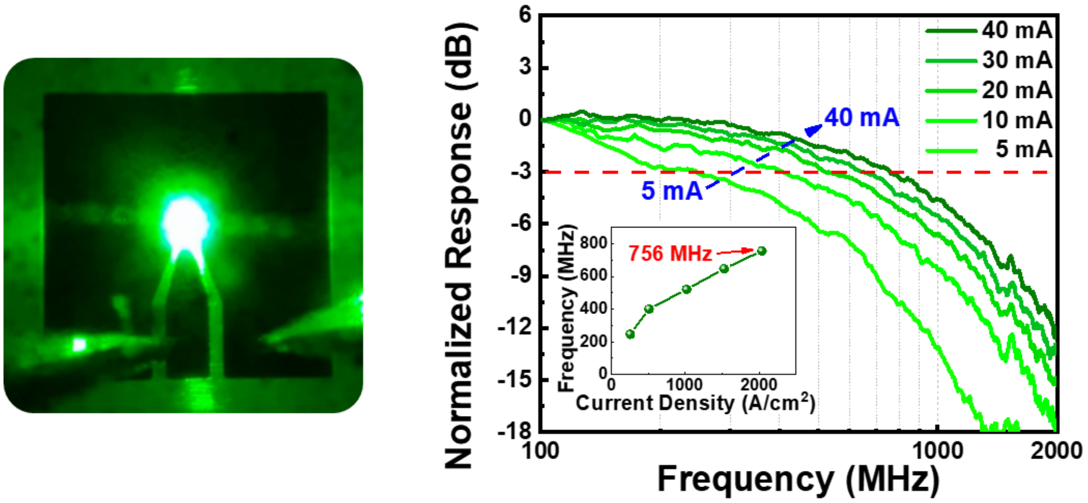

50-µm semipolar micro-LED and its frequency response performance.